

# Peptide Self-Assembly on Mica under Ethanol-Containing Atmospheres: Effects of Ethanol on Epitaxial Growth of Peptide Nanofilaments

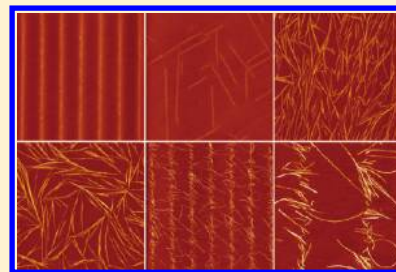
Muyun Xie,<sup>†,‡</sup> Hai Li,<sup>†</sup> Ming Ye,<sup>†</sup> Yi Zhang,<sup>\*,†</sup> and Jun Hu<sup>\*,†</sup>

<sup>†</sup>Shanghai Institute of Applied Physics, Chinese Academy of Sciences

<sup>‡</sup>Graduate School of the Chinese Academy of Sciences

## S Supporting Information

**ABSTRACT:** Our previous study has shown that the self-assembly of several neurodegenerative-disease-related peptides in ambient water nanofilm condensed on mica is very sensitive to the amount of water on the surface. In this paper, we will demonstrate our hypothesis that the introduction of ethanol into the water nanofilm alters the properties of the interfacial water, resulting in changes of the peptide nanostructures self-assembled on the substrate. The assembly behaviors of peptides under different ethanol-containing atmospheres on mica were investigated by atomic force microscopy. GAV-9a began to form bent nanofilaments under an ethanol-containing atmosphere, and the self-assembled nanofilaments became thicker when a higher ratio of ethanol to water in the vapor was used. Based on these results, we propose a possible mechanism that the peptides adopt a “tilted upright” orientation when ethanol is present in the incubation environment. The effect of the peptide’s terminal groups on the self-assembled nanostructures under the ethanol-containing atmosphere was also discussed.



## ■ INTRODUCTION

In the past years the self-assembly of peptides has attracted a great deal of attention owing to its potential in the formation of novel nanostructures,<sup>1–23</sup> which are well-suited for many promising applications, such as nanofluidic devices,<sup>1</sup> fabrication of metallic nanowires<sup>2,3</sup> and coaxial nanocables,<sup>4</sup> scaffolds of tissue,<sup>5,6</sup> drug delivery,<sup>7–10</sup> and biosensors.<sup>11–13</sup> The peptide self-assembly process can be modulated by using a variety of environmental triggers, such as pH,<sup>24–32</sup> ionic strength,<sup>26,33</sup> metal ions,<sup>34–36</sup> temperature,<sup>37,38</sup> and oxidative stress,<sup>39</sup> which allows the fabrication of peptide-based nanostructures with designated functions. Among them are a variety of solid substrates which play important roles during peptide self-assembly, and it has been found that some substrates may act as templates to direct peptide self-assembly at the surface,<sup>21–23,40–43</sup> which provides a powerful approach for fabrication of ordered peptide nanostructures.

Peptide self-assembly on surfaces is also influenced by interfacial water molecules condensed from the environment.<sup>44</sup> Interfacial water is believed to widely exist in biological systems,<sup>45</sup> and its biological functions have been studied by employing models such as reverse micelles,<sup>46–53</sup> proteins,<sup>54–61</sup> and Nafion fuel cell membranes.<sup>62,63</sup> Previously, we have used the water nanofilm on mica<sup>64–67</sup> as a model system to study the effects of confined water on the self-assembly behaviors of peptides. It was observed that the peptide showed different epitaxial self-assembling behaviors at relative humidity above 45%,<sup>44</sup> according to which a self-assembly model that describes

the peptide arrangement in the confined water nanofilm was proposed.<sup>68</sup>

However, a comprehensive understanding of the role the interfacial water plays in the peptide self-assembly is still not available. Studying the self-assembly behaviors of peptides in altered interfacial water environments by introducing cosolvents may be a feasible approach toward a better understanding of the self-assembly mechanism.<sup>69</sup> One of the most commonly used cosolvents is alcohol. Alcohol–water mixtures have been used as model solvents in various biological studies to investigate the effects of solvents on proteins,<sup>70–77</sup> and it has been reported that the addition of alcohols induces the aggregation of proteins.<sup>78–80</sup> For example, it has been found that ethanol accelerates the aggregation of insulin, and increasing the concentration of ethanol promotes the formation of curved, amorphous, and finally donut-shaped aggregates.<sup>78</sup> The effects of alcohols have partially been attributed to the ordering of the solvent structure, lowering the dielectric constant of the solvent, hydrophobic effects, changes in hydrogen bonding along the peptide chain, or the combination of these influences.<sup>74</sup> Although it has been demonstrated that alcohols bind directly to proteins, it is believed that alcohols affect protein structure mainly through solvent effects.<sup>73</sup>

We hypothesize that by introducing ethanol into the experimental system, the water nanofilm confined on a mica

**Received:** September 15, 2011

**Revised:** January 19, 2012

**Published:** February 14, 2012



surface would be altered as ethanol is miscible with water. Therefore, the self-assembly of the peptide in such a system should strongly depend on the presence of ethanol. Herein, we demonstrated this hypothesis by monitoring the growth of peptide nanofilaments in the ethanol-altered interfacial water nanofilm.

## MATERIALS AND METHODS

**Peptides Sample Preparation.** GAV-9 ( $\text{NH}_2\text{-VGGAV-VAGV-CONH}_2$ ) and GAV-9a ( $\text{CH}_3\text{CONH-VGGAV-VAGV-CONH}_2$ ) were both synthesized by using the Boc solid-phase method on an ABI 433 A peptide synthesizer (Applied Biosystems) and cleaved from the MBHA resin (100–200 mesh, Fluka) with hydrogen fluoride. These peptides were purified through a TSK-40 (S) column (2.0 cm  $\times$  98 cm, Tosoh). Ethanol (HPLC grade) was purchased from Fisher. Before use, the peptides were dissolved in Milli-Q water to a final concentration of 1 mg/mL.

**Microcontact Printing ( $\mu\text{CP}$ ).** Peptides were patterned and deposited on a freshly cleaved mica substrate with a  $\mu\text{CP}$  method in a dry environment. The PDMS stamps were fabricated by casting a 10:1 (w:w) mixture of Sylgard 184 elastomer/curing agent (Dow Corning) against a master with 1.6  $\mu\text{m}$  pitch on its surface and heating at 70  $^\circ\text{C}$  for 12 h after degassing. The stamp was coated with peptide by dipping it into the peptide solution for about 2 min, followed by drying it under a stream of nitrogen gas. The peptide was transferred onto substrate surface by placing the stamp on a freshly cleaved mica sheet with a gentle press for about 30 s. The whole processes were carried out at temperature of  $\sim 20$   $^\circ\text{C}$  and relative humidity of  $\sim 40\%$  or less.

**Atmosphere Control during Sample Incubation.** Samples with peptide patterns on the surface were placed in a sealed box with a volume of  $\sim 1$  L. At least one-fifth of the total volume was filled with a certain concentration of ethanol aqueous solution to guarantee an equilibrium vapor pressure of ethanol in the sealed environment. Then the samples were incubated in the box for a time period of  $\sim 20$  h at 20  $^\circ\text{C}$ . The equilibrium pressures of ethanol and water vapors in the box were regulated by using ethanol solutions with different concentrations. The mole fractions of ethanol in liquid and in vapor corresponding to every incubation condition are listed in Table 1.

**Table 1. Vapor–Liquid Equilibrium Data for Ethanol–Water at 298.15 K<sup>a</sup>**

vol. fraction of ethanol in liquid (%)	mole fraction of ethanol in liquid (%)	mole fraction of ethanol in vapor (%)	vol. fraction of ethanol in vapor (%)
0	0	0	0
10	3.3	25.9	53.1
50	23.6	54.6	79.6
100	100	100	100

<sup>a</sup>Obtained from ref 82.

**Atomic Force Microscopy.** A commercial atomic force microscope (AFM) (Nanoscope IIIa, Veeco) equipped with an E-scanner was employed, and the tapping mode in air was performed. Silicon cantilevers with spring constants of 2–20 N  $\text{m}^{-1}$  (NSG 11, NT-MDT) and 48 N  $\text{m}^{-1}$  (NSC 11,  $\mu\text{Masch}$ ) were used. AFM imaging was conducted in air at room temperature and RH of  $\sim 40\%$  or less.

## RESULTS AND DISCUSSION

In our experiment, mica substrates with patterned peptides were incubated under equilibrium atmospheres containing different fractions of ethanol and water vapors (see Table 1).

Since the self-assembly of GAV-9a peptide on mica is very sensitive to the water environment around, we first studied the influence of ethanol on its assembly behavior. As shown in Figure 1, AFM observation revealed details of GAV-9a nanostructures formed under different atmospheres. When incubated in a water-vapor-saturated environment, GAV-9a self-assembled into straight nanofilaments (Figure 1B) which were arranged either in parallel or at 60 $^\circ$  to each other, a direct evidence of epitaxy on mica.<sup>44</sup> The nanofilaments have a height of  $\sim 0.4$  nm (Figure 1F), corresponding to a single layer of peptide in a  $\beta$ -sheet conformation with peptide “lying down” on the surface.<sup>44</sup> However, when incubated under an atmosphere generated by a 10% ethanol solution, most of the GAV-9a molecules preferred to form bent nanofilaments with a thickness of  $\sim 0.9$  nm (Figure 1C and G), indicating a lesser degree of epitaxy on mica. The peptide nanostructures became thicker (1–2 nm, Figure 1D, G, and H) when the concentration of ethanol solution presented in the incubation environment increased to 50%. Finally, when the peptide was incubated in a pure ethanol environment, many more curved nanofilaments (Figure 1E and 1F) with thickness of 1–3 nm were formed (Figure 1G and I).

The diffusion and assembly processes of the peptide on the mica substrates have been investigated with AFM. Results indicated that the GAV-9a molecules diffuse quickly under the atmospheres maintained with water and aqueous solutions of ethanol. For example, as shown in Figure 2, the peptides diffuse from initial strips to an adjacent area and form nanofilaments in less than several hours under the atmosphere maintained with 10% ethanol solution. The newly formed peptide nanofilaments might be in a dynamic equilibrium as some small filaments disappeared while some others appeared at different locations. A similar phenomenon was observed under the atmosphere maintained with 50% ethanol solution (data not shown).

Although the ethanol molecules may bind directly to the peptide molecules during the self-assembly process,<sup>78</sup> it is not considered to be the main factor causing the structural changes of the peptide. This inference is supported by the fact that the heights of the nanofilaments would not reduce after further incubation in low relative humidity environments, in which ethanol molecules would evaporate. Instead, in our opinion, the influence of ethanol atmosphere on the peptide nanostructures should be attributed to the changes in properties of the interfacial water nanofilm which plays an important role in the substrate-directed peptide self-assembly.<sup>44</sup> In a pure water-vapor environment, GAV-9a tended to form flat nanofilaments to ensure a maximal contact between the hydrophobic peptide and the hydrophobic vapor/water interface. When ethanol-containing atmospheres were used, ethanol molecules were also adsorbed at the vapor/liquid interface. The formation of flat nanofilaments at the water nanofilm was blocked, and GAV-9a preferred to self-assemble into bent nanofilaments.

The thickness increase of the peptide filaments along with the increasing of the ethanol vapor pressure in the incubation environment may be explained with a “tilted upright” model (Figure 3). Under these incubation conditions, ethanol molecules were condensed along with the condensation of water on the mica surface, as has been revealed by a vibrating

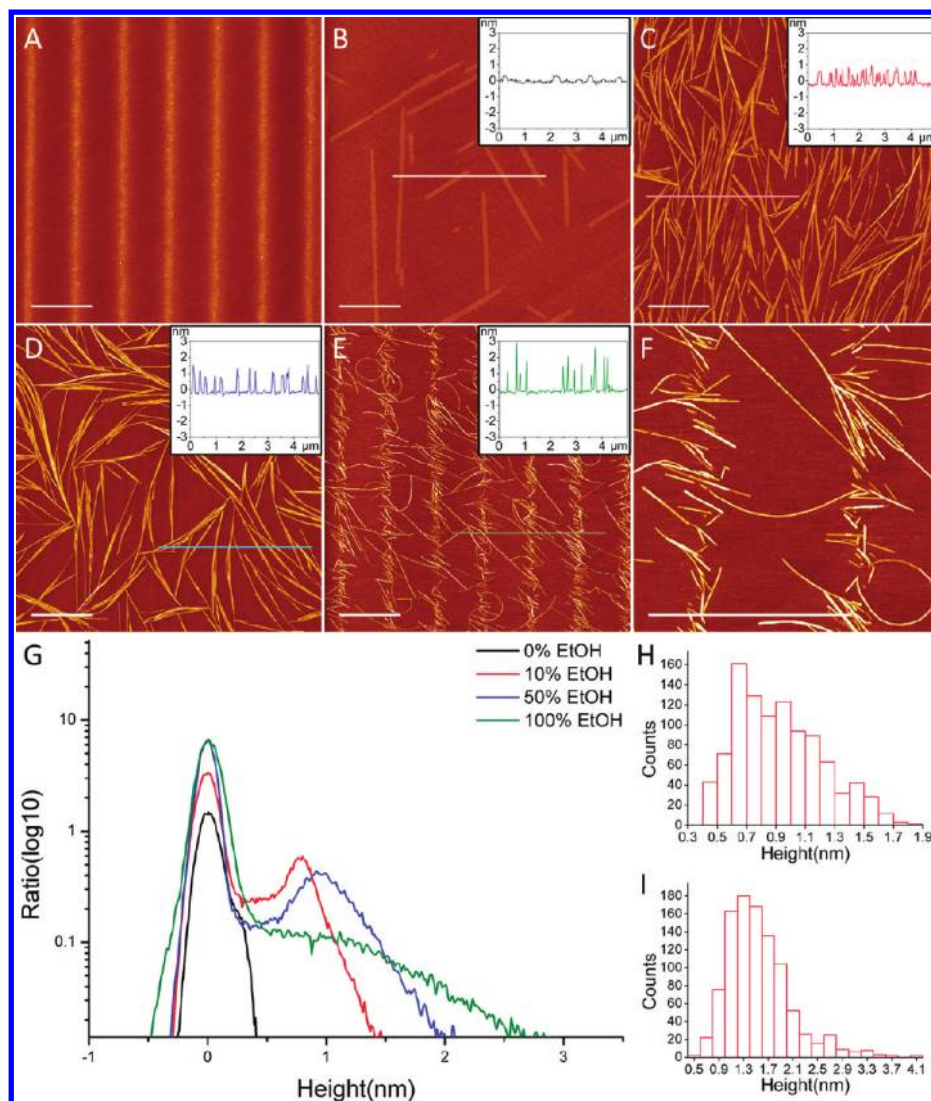


**Figure 1.** AFM images of self-assembled GAV-9a nanostructures under ethanol/water atmospheres on mica surface. All the samples were incubated at 20 °C for 20 h. (A) Representative image of peptide pattern before incubation. (B–E) AFM images of peptide nanostructures formed under different atmospheres, which were maintained with aqueous solutions of ethanol with volume fractions of 0% (B), 10% (C), 50% (D), and 100% (E and F), respectively. Insets: section analyses of the lines marked on the pictures. Scale bars represent 2000 nm. (G) Typical height distribution curves of GAV-9a nanostructures formed in different incubation environments. Each curve was generated by the software Origin with the X–Z data of a selected AFM image from the AFM software using the command “Depth”. The peak at 0 nm of each curve represents the surface of mica. The y-axis was set to a logarithmic scale for convenience of observation. (H–I) Histograms showing the thickness distribution of GAV-9a nanofilaments formed under 50% (H) and 100% (I) ethanol atmospheres, respectively. The peptide nanostructures that were piled up with each other were excluded from these statistics.

scanning polarization force microscopy.<sup>81</sup> The presence of the large amount of ethanol in the water nanofilm compressed the surface area on which the peptide molecules were self-assembled; thus, GAV-9a peptide forming the nanofilaments may turn to adopt a tilted upright orientation (Figure 3B and C). In this model, the contact area of the peptide with the vapor/liquid interface was reduced and the epitaxial relationship with underlying mica lattice was crippled, which led to the formation of bent nanofilaments. When the volume fraction of ethanol in the incubation environment was relatively low, the peptides tilted to a lesser degree and the heights of most nanofilaments were less than 1 nm. Then, after the amount of introduced ethanol molecules increased, the tilting angle became larger and the nanofilaments became thicker. Finally, when a pure ethanol atmosphere was used, the orientation of

some nanofilaments was close to “upright”, with a thickness of almost the length of a peptide molecule (3 nm).

Another explanation of the above results one may consider relies on a “desorption” model. In this model, ethanol molecules out-compete peptide molecules for adsorption sites at the liquid–vapor interface, and as the concentration of ethanol increases, a large number of peptide molecules are desorbed from mica surface. However, if it is the case, the desorbed peptide should form random aggregates, not only the filament structures that we have observed.

Since the epitaxial relationship between the peptide and the underlying mica substrate was weakened when a pure ethanol environment was used, it seemed reasonable that the “lying down”-oriented nanofilaments formed in a water-vapor environment could also be inverted to higher tilted upright nanofilaments. To confirm this speculation, incubation environ-



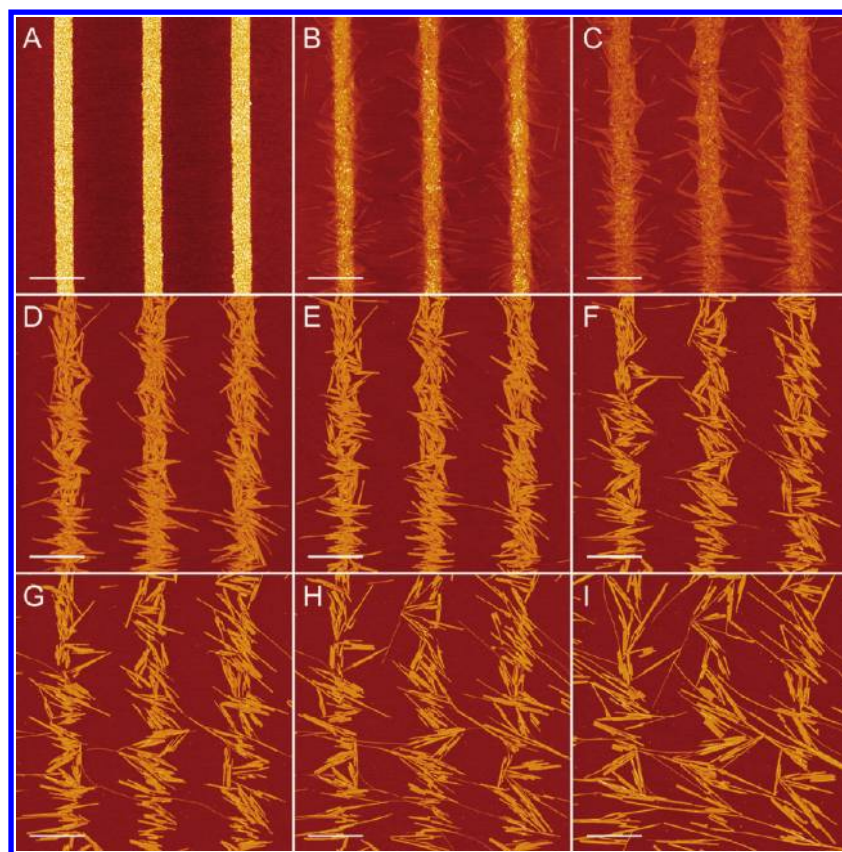


**Figure 2.** Series of AFM images indicating the diffusion and assembly processes of GAV-9a under the atmosphere maintained by a 10% ethanol solution after incubated for 0 (A), 7 (B), 15 (C), 30 (D), 60 (E), 150 (F), 300 (G), 600 (H), and 1200 (I) min, respectively. Scale bars represent 1000 nm.

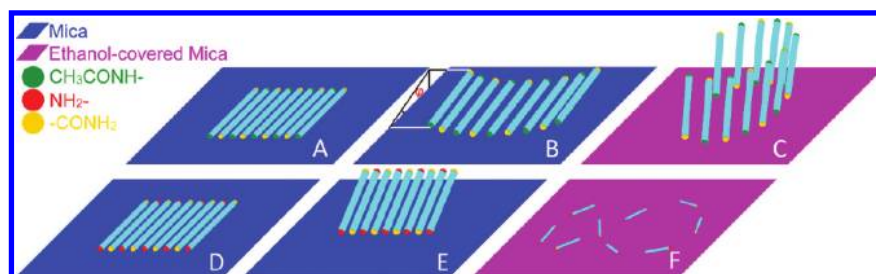


**Figure 3.** Schematic representation of the possible nanostructures of GAV-9a and GAV-9 formed under ethanol/water atmospheres. (A) GAV-9a nanostructures in a saturated RH environment. (B) GAV-9a nanostructures in ethanol-containing environments. (C) GAV-9a nanostructures in a pure ethanol environment. (D) GAV-9 nanostructures in water-dominated environments. (E) GAV-9 nanostructures in ethanol-dominated environments. (F) GAV-9 nanostructures in a pure ethanol environment.  $\varphi$ : tilting angle.

ment switch experiments were performed. As shown in Figure 4A1, straight GAV-9a nanofilaments with threefold symmetry were formed after being incubated at RH 70%. After further incubation in an ethanol environment for the same time period (Figure 4A2), most of the straight nanofilaments disappeared. Instead, thicker bent nanofilaments appeared on the substrate, which indicated that the peptide adopted a tilted upright orientation. When the samples of GAV-9a nanofilaments generated by pure water vapor were further incubated for a long time under an ethanol atmosphere, almost all the nanofilaments could be reassembled into long thicker nanofilaments (Figure 4B2).

Interestingly, the reassembly process is reversible by exchanging the incubating condition. As shown in Figure 4C, under a high RH environment the thick nanofilaments, which

were formed with tilted upright peptide molecules in an ethanol environment, were unstable and partly transformed to thinner epitaxially oriented nanofilaments. When the incubation time was extended, almost all the thicker bent nanofilaments were reassembled into straight epitaxial nanofilaments (Figure 4D1 and D2).

To test the effects of the peptide end groups on the peptide self-assembly behaviors under different incubation atmospheres, similar incubating experiments were performed on the peptide GAV-9. It seemed that the introduction of ethanol molecules in the vapor also led to changes of the GAV-9 nanofilaments, as revealed by the AFM observation (Figure 5). The GAV-9 molecules self-assembled into ordered epitaxial nanofilaments when incubated in a saturated RH environment (Figure 5B). When the 10% ethanol solution was used for

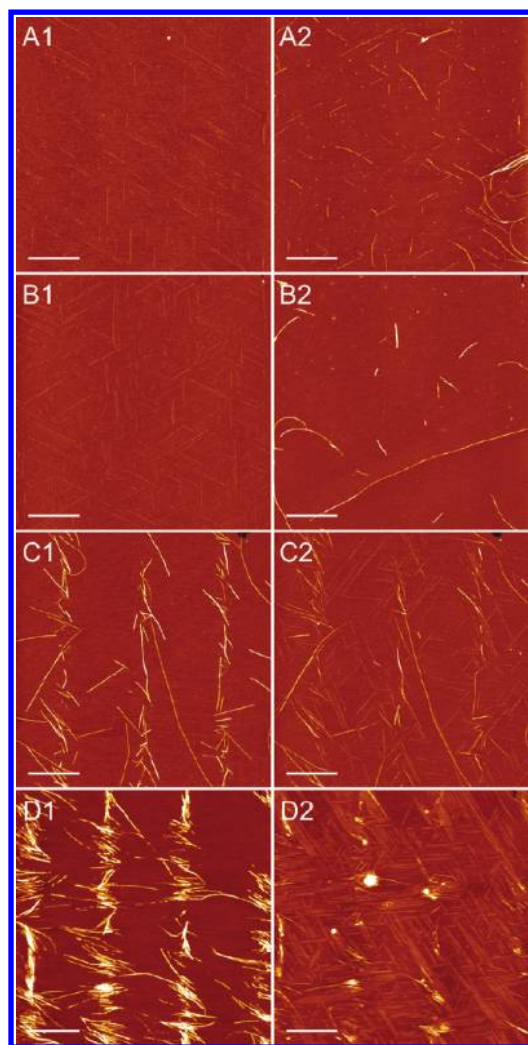


**Figure 4.** AFM observation of GAV-9a nanofilaments formed in environment-switching experiments. Experiment I: The GAV-9a samples were incubated in RH 70% for 20 h first (A1 and B1) and then in 100% ethanol atmosphere for 20 h (A2) and 90 h (B2), respectively. Experiment II: The GAV-9a samples were incubated in 100% ethanol atmosphere for 20 h first (C1 and D1) and then in RH 70% for 20 h (C2) and 80 h (D2), respectively. Scale bars represent 1000 nm.

controlling the incubation environment, the GAV-9 peptides assembled into ordered epitaxial nanofilaments too and there seemed to be no obvious difference (Figure 5C). However, the assembled nanofilaments would be thicker when a higher concentration of ethanol (e.g., 50%) was used (Figure 5D). The thicker nanofilaments could still be obtained even if the volume proportion of ethanol increased up to 95%. The epitaxial growth of GAV-9 was not interrupted until a pure ethanol atmosphere was used, which resulted in very short fibrils randomly deposited on the mica substrate (Figure 5E and F).

The response of the GAV-9 on the ethanol-containing atmosphere is obviously different from the GAV-9a. Unlike the GAV-9a, the N terminal of GAV-9 is positively charged; thus, the electrostatic interaction between the N terminal of the peptide and the negatively charged mica substrate becomes the determinant factor in the self-assembly process. This electrostatic interaction can also be the origin of the epitaxial arrangement of the nanofilaments on the mica surface. When GAV-9 molecules form nanofilaments in a pure water

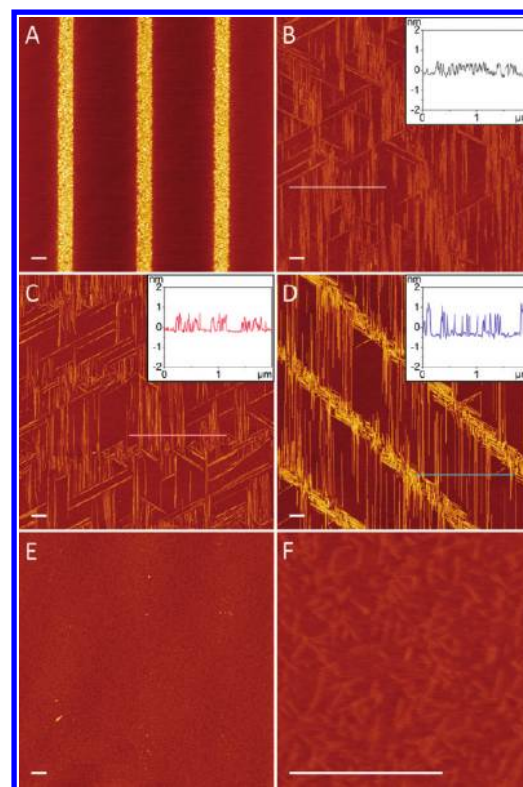


**Figure 5.** AFM images of self-assembled GAV-9 nanofilaments under ethanol/water atmospheres on mica surface. All the samples were incubated at 20 °C for 20 h. (A) Representative image of peptide pattern before incubation. (B–F) AFM images of peptide nanostructures formed under different atmospheres, which were maintained with aqueous solutions of ethanol with volume fractions of 0% (B), 10% (C), 50% (D), and 100% (E and F), respectively. Insets: section analyses of the lines marked on the pictures. Scale bars represent 300 nm.

environment,<sup>44</sup> the positively charged N terminals strongly interact with negatively charged mica surface, making the peptide “lying down” and the assembled nanofilaments anchored close to the substrate (Figure 3D). As the electrostatic interaction can stabilize the lying down orientation of the peptide, the substrate-directed self-assembly could still be carried out when the mole fraction of ethanol in vapor reached 25% (maintained by 10% ethanol solution). When the ethanol concentration increased to 50% or more, the mole fraction of ethanol in vapor reached 50% or higher (Table 1), resulting in a vapor/liquid interface on the mica substrate which was mainly occupied by the ethanol molecules. Thus, a tilted upright orientation of the peptide was adopted (Figure 3E), while the consistency with the underlying atomic lattice of mica substrate could still be maintained by the electrostatic interaction. At last, when a pure ethanol atmosphere was used, ethanol film was formed on mica surface.<sup>81</sup> As ethanol is a nonelectrolyte, the electrostatic interaction between the N terminal of the peptide and the mica substrate was minimized, and eventually the intermolecular interaction between peptide molecules became the determinant factor during peptide assembly, resulting in randomly arranged nanofilaments (Figure 3F).

Incubation environment switch experiments were also performed. Similar to GAV-9a, when the incubation atmosphere was switched from a saturated ethanol vapor to a saturated water vapor, the randomly arranged nanofilaments



were not stable, and the epitaxial self-assembly of GAV-9 was resumed (Figure 6A). However, the highly ordered GAV-9

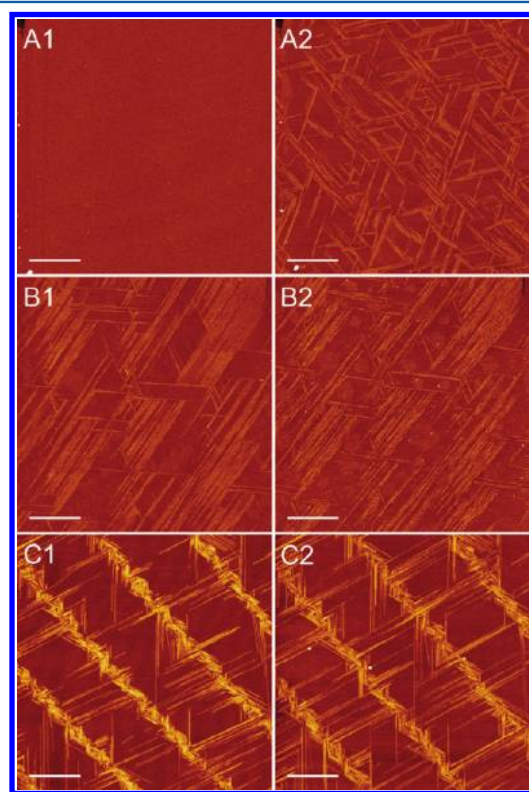


**Figure 6.** AFM observation of GAV-9 nanofilaments formed in environment-switching experiments. (A1) GAV-9 nanofilaments formed in 100% ethanol atmosphere. (A2) Same sample of A1 after further incubation in 100% RH. (B1) GAV-9 nanofilaments formed in 100% RH. (B2) Same sample of B1 after further incubation in 100% ethanol atmosphere. (C1) GAV-9 nanofilaments formed in atmosphere provided with 50% ethanol solution. (C2) Same sample of C1 after further incubation in 100% ethanol atmosphere. Each incubation time period is 20 h. Scale bars represent 1000 nm.

nanofilaments, once formed on the surface, were very stable in a pure ethanol environment. As shown in Figure 6B and C, most epitaxially arranged nanofilaments were unaltered after being further incubated under a pure ethanol atmosphere for 20 h. The difference in stability between GAV-9 and GAV-9a nanostructures under a saturated ethanol atmosphere could be ascribed to the fact that the substrate-directed growth of GAV-9 nanofilaments is determined by the electrostatic interaction, while the epitaxial self-assembly process of GAV-9a depends mainly on the hydrophobic interaction between the hydrophobic peptide and the hydrophobic vapor/water interface.<sup>68</sup>

## CONCLUSIONS

In summary, we have demonstrated our hypothesis that the introduction of ethanol into the water nanofilm confined on mica substrate alters the properties of the interfacial water, resulting in changes of the peptide nanostructures self-assembled on the substrate. GAV-9a began to form bent nanofilaments under an ethanol-containing atmosphere and the self-assembled nanofilaments became thicker when a higher ratio of ethanol to water in the vapor was used. Based on these results, we propose a possible mechanism that the peptides adopt a tilted upright orientation when ethanol is present in the

incubation environment. Moreover, it was found that nanostructures formed with different peptides showed different stabilities when ethanol molecules were introduced. The nanostructures of acylamino-terminated GAV-9a in a lying down orientation were sensitive to ethanol vapor; in sharp contrast, the nanofilaments of amino-terminated GAV-9 showed a high degree of stability in a pure ethanol environment, which may be ascribed to the electrostatic interaction between the positively charged N terminal groups and the mica substrate. Our finding that the structures of peptides could be regulated by using an ethanol-containing atmosphere may be potentially useful in nanomanufacturing applications.

## ASSOCIATED CONTENT

### Supporting Information

CD spectra of GAV-9 solutions and AFM images of GAV-9 nanofilaments formed by peptide strips with different heights. This material is available free of charge via the Internet at <http://pubs.acs.org>.

## AUTHOR INFORMATION

### Corresponding Author

\*Tel.: 86-21-39194607. Fax: 86-21-59552394. E-mail: [zhangyi@sinap.ac.cn](mailto:zhangyi@sinap.ac.cn) (Y.Z.), [hujun@sinap.ac.cn](mailto:hujun@sinap.ac.cn) (J.H.).

### Notes

The authors declare no competing financial interest.

## ACKNOWLEDGMENTS

This work was supported by grants from the Chinese Academy of Sciences, the National Science Foundation of China (No. 10975175 and 90923002), and the National Basic Research Program of China (No. 2007CB936000). Y.Z. thanks the Max Planck Society for support of a partner group.

## REFERENCES

- (1) Adler-Abramovich, L.; Aronov, D.; Beker, P.; Yevnin, M.; Stempler, S.; Buzhansky, L.; Rosenman, G.; Gazit, E. *Nat. Nanotechnol.* **2009**, *4*, 849–854.
- (2) Scheibel, T. *Proc. Natl. Acad. Sci. U.S.A.* **2003**, *100*, 4527–4532.
- (3) Reches, M. *Science* **2003**, *300*, 625–627.
- (4) Carny, O.; Shalev, D. E.; Gazit, E. *Nano Lett.* **2006**, *6*, 1594–1597.
- (5) Ellis-Behnke, R. G. *Proc. Natl. Acad. Sci. U.S.A.* **2006**, *103*, 5054–5059.
- (6) Yokoi, H. *Proc. Natl. Acad. Sci. U.S.A.* **2005**, *102*, 8414–8419.
- (7) Lim, Y.-b.; Lee, E.; Lee, M. *Angew. Chem., Int. Ed.* **2007**, *46*, 3475–3478.
- (8) Mahler, A.; Reches, M.; Rechter, M.; Cohen, S.; Gazit, E. *Adv. Mater.* **2006**, *18*, 1365–1370.
- (9) Naskar, J.; Palui, G.; Banerjee, A. *J. Phys. Chem. B* **2009**, *113*, 11787–11792.
- (10) Li, X.; Li, J.; Gao, Y.; Kuang, Y.; Shi, J.; Xu, B. *J. Am. Chem. Soc.* **2010**, *132*, 17707–17709.
- (11) Yemini, M.; Reches, M.; Rishpon, J.; Gazit, E. *Nano Lett.* **2005**, *5*, 183–186.
- (12) Yang, H.; Fung, S.-Y.; Pritzker, M.; Chen, P. *Langmuir* **2009**, *25*, 7773–7777.
- (13) Xu, H.; Das, A. K.; Horie, M.; Shaik, M. S.; Smith, A. M.; Luo, Y.; Lu, X.; Collins, R.; Liem, S. Y.; Song, A.; Popelier, P. L. A.; Turner, M. L.; Xiao, P.; Kinloch, I. A.; Ulijn, R. V. *Nanoscale* **2010**, *2*, 960–966.
- (14) Adhikari, B.; Banerjee, A. *Chem.—Eur. J.* **2010**, *16*, 13698–13705.
- (15) Lashuel, H. A.; LaBrenz, S. R.; Woo, L.; Serpell, L. C.; Kelly, J. W. *J. Am. Chem. Soc.* **2000**, *122*, 5262–5277.

- (16) Zhang, S.; Marini, D. M.; Hwang, W.; Santoso, S. *Curr. Opin. Chem. Biol.* **2002**, *6*, 865–871.
- (17) Zhang, S. *Nat. Biotechnol.* **2003**, *21*, 1171–1178.
- (18) Vauthey, S. *Proc. Natl. Acad. Sci. U.S.A.* **2002**, *99*, 5355–5360.
- (19) Fairman, R.; Akerfeldt, K. *Curr. Opin. Struct. Biol.* **2005**, *15*, 453–463.
- (20) Hentschel, J.; Börner, H. G. *J. Am. Chem. Soc.* **2006**, *128*, 14142–14149.
- (21) Whitehouse, C.; Fang, J.; Aggeli, A.; Bell, M.; Brydson, R.; Fishwick, C. W. G.; Henderson, J. R.; Knobler, C. M.; Owens, R. W.; Thomson, N. H.; Smith, D. A.; Boden, N. *Angew. Chem., Int. Ed.* **2005**, *44*, 1965–1968.
- (22) Zhang, F.; Du, H.-N.; Zhang, Z.-X.; Ji, L.-N.; Li, H.-T.; Tang, L.; Wang, H.-B.; Fan, C.-H.; Xu, H.-J.; Zhang, Y.; Hu, J.; Hu, H.-Y.; He, J.-H. *Angew. Chem., Int. Ed.* **2006**, *45*, 3611–3613.
- (23) Yang, H.; Fung, S.-Y.; Pritzker, M.; Chen, P. *Angew. Chem., Int. Ed.* **2008**, *47*, 4397–4400.
- (24) Pagel, K.; Wagner, S. C.; Samedov, K.; von Berlepsch, H.; Böttcher, C.; Koks, B. *J. Am. Chem. Soc.* **2006**, *128*, 2196–2197.
- (25) Zimenkov, Y.; Dublin, S. N.; Ni, R.; Tu, R. S.; Breedveld, V.; Apkarian, R. P.; Conticello, V. P. *J. Am. Chem. Soc.* **2006**, *128*, 6770–6771.
- (26) Dong, H.; Paramonov, S. E.; Aulisa, L.; Bakota, E. L.; Hartgerink, J. D. *J. Am. Chem. Soc.* **2007**, *129*, 12468–12472.
- (27) Bose, P. P.; Das, A. K.; Hegde, R. P.; Shamala, N.; Banerjee, A. *Chem. Mater.* **2007**, *19*, 6150–6157.
- (28) Verel, R.; Tomka, I. T.; Bertozzi, C.; Cadalbert, R.; Kammerer, R. A.; Steinmetz, M. O.; Meier, B. H. *Angew. Chem., Int. Ed.* **2008**, *47*, 5842–5845.
- (29) Shera, J. N.; Sun, X. S. *Biomacromolecules* **2009**, *10*, 2446–2450.
- (30) Rajagopal, K.; Lamm, M. S.; Haines-Butterick, L. A.; Pochan, D. J.; Schneider, J. P. *Biomacromolecules* **2009**, *10*, 2619–2625.
- (31) Cui, H.; Muraoka, T.; Cheetham, A. G.; Stupp, S. I. *Nano Lett.* **2009**, *9*, 945–951.
- (32) Deng, M.; Yu, D.; Hou, Y.; Wang, Y. *J. Phys. Chem. B* **2009**, *113*, 8539–8544.
- (33) Castelletto, V.; Hamley, I. W.; Cenker, C.; Olsson, U. *J. Phys. Chem. B* **2010**, *114*, 8002–8008.
- (34) Zou, J.; Kajita, K.; Sugimoto, N. *Angew. Chem., Int. Ed.* **2001**, *40*, 2274–2277.
- (35) Futaki, S.; Kiwada, T.; Sugiura, Y. *J. Am. Chem. Soc.* **2004**, *126*, 15762–15769.
- (36) Cerasoli, E.; Sharpe, B. K.; Woolfson, D. N. *J. Am. Chem. Soc.* **2005**, *127*, 15008–15009.
- (37) Liu, X.; Zhang, Y.; Goswami, D. K.; Okasinski, J. S.; Salaita, K.; Sun, P.; Bedzyk, M. J.; Mirkin, C. A. *Science* **2005**, *307*, 1763–1766.
- (38) Kammerer, R. A. *Proc. Natl. Acad. Sci. U.S.A.* **2004**, *101*, 4435–4440.
- (39) Siegel, S. J.; Bieschke, J.; Powers, E. T.; Kelly, J. W. *Biochemistry* **2007**, *46*, 1503–1510.
- (40) Kowalewski, T.; Holtzman, D. M. *Proc. Natl. Acad. Sci. U.S.A.* **1999**, *96*, 3688–3693.
- (41) Brown, C. L.; Aksay, I. A.; Saville, D. A.; Hecht, M. H. *J. Am. Chem. Soc.* **2002**, *124*, 6846–6848.
- (42) Yang, G.; Woodhouse, K. A.; Yip, C. M. *J. Am. Chem. Soc.* **2002**, *124*, 10648–10649.
- (43) Zhang, F.-C.; Zhang, F.; Su, H.-N.; Li, H.; Zhang, Y.; Hu, J. *ACS Nano* **2010**, *4*, 5791–5796.
- (44) Li, H.; Zhang, F.; Zhang, Y.; Ye, M.; Zhou, B.; Tang, Y.-Z.; Yang, H.-J.; Xie, M.-Y.; Chen, S.-F.; He, J.-H.; Fang, H.-P.; Hu, J. *J. Phys. Chem. B* **2009**, *113*, 8795–8799.
- (45) Ball, P. *Chem. Rev.* **2008**, *108*, 74–108.
- (46) Faeder, J.; Ladanyi, B. M. *J. Phys. Chem. B* **2000**, *104*, 1033–1046.
- (47) Angulo, G.; Organero, J. A.; Carranza, M. A.; Douhal, A. *J. Phys. Chem. B* **2006**, *110*, 24231–24237.
- (48) Douhal, A.; Angulo, G.; Gil, M.; Organero, J. Á.; Sanz, M.; Tormo, L. *J. Phys. Chem. B* **2007**, *111*, 5487–5493.
- (49) Choudhury, S. D.; Nath, S.; Pal, H. *J. Phys. Chem. B* **2008**, *112*, 7748–7753.
- (50) Biswas, R.; Rohman, N.; Pradhan, T.; Buchner, R. *J. Phys. Chem. B* **2008**, *112*, 9379–9388.
- (51) Mukhopadhyay, M.; Mandal, A.; Misra, R.; Banerjee, D.; Bhattacharyya, S. P.; Mukherjee, S. *J. Phys. Chem. B* **2009**, *113*, 567–573.
- (52) Heisler, I. A.; Kondo, M.; Meech, S. R. *J. Phys. Chem. B* **2009**, *113*, 1623–1631.
- (53) Park, S.-Y.; Kwon, O.-H.; Kim, T. G.; Jang, D.-J. *J. Phys. Chem. C* **2009**, *113*, 16110–16115.
- (54) Pal, S. K.; Zewail, A. H. *Chem. Rev.* **2004**, *104*, 2099–2124.
- (55) Peon, J. *Proc. Natl. Acad. Sci. U.S.A.* **2002**, *99*, 10964–10969.
- (56) Pal, S. K. *Proc. Natl. Acad. Sci. U.S.A.* **2002**, *99*, 15297–15302.
- (57) Bandyopadhyay, S.; Chakraborty, S.; Balasubramanian, S.; Bagchi, B. *J. Am. Chem. Soc.* **2005**, *127*, 4071–4075.
- (58) Russo, D.; Murarka, R. K.; Copley, J. R. D.; Head-Gordon, T. *J. Phys. Chem. B* **2005**, *109*, 12966–12975.
- (59) Daidone, I.; Ulmschneider, M. B.; Di Nola, A.; Amadei, A.; Smith, J. C. *Proc. Natl. Acad. Sci. U.S.A.* **2007**, *104*, 15230–15235.
- (60) Zhang, L.; Wang, L.; Kao, Y. T.; Qiu, W.; Yang, Y.; Okobiah, O.; Zhong, D. *Proc. Natl. Acad. Sci. U.S.A.* **2007**, *104*, 18461–18466.
- (61) Ebbinghaus, S.; Kim, S. J.; Heyden, M.; Yu, X.; Heugen, U.; Gruebele, M.; Leitner, D. M.; Havenith, M. *Proc. Natl. Acad. Sci. U.S.A.* **2007**, *104*, 20749–20752.
- (62) Moilanen, D. E.; Piletic, I. R.; Fayer, M. D. *J. Phys. Chem. C* **2007**, *111*, 8884–8891.
- (63) Spry, D. B.; Goun, A.; Glusac, K.; Moilanen, D. E.; Fayer, M. D. *J. Am. Chem. Soc.* **2007**, *129*, 8122–8130.
- (64) Verdaguer, A.; Sacha, G. M.; Bluhm, H.; Salmeron, M. *Chem. Rev.* **2006**, *106*, 1478–1510.
- (65) Ewing, G. E. *Chem. Rev.* **2006**, *106*, 1511–1526.
- (66) Hu, J.; Xiao, X.-D.; Ogletree, D. F.; Salmeron, M. *Science* **1995**, *268*, 267–269.
- (67) Odelius, M.; Bernasconi, M.; Parrinello, M. *Phys. Rev. Lett.* **1997**, *78*, 2855–2858.
- (68) Ye, M.; Zhang, Y.; Li, H.; Xie, M.; Hu, J. *J. Phys. Chem. B* **2010**, *114*, 15759–15765.
- (69) Neuman, R. C.; Gerig, J. T. *J. Phys. Chem. B* **2011**, *115*, 1712–1719.
- (70) Chaudhary, N.; Singh, S.; Nagaraj, R. *Biopolymers* **2008**, *90*, 783–791.
- (71) Chaudhary, N.; Singh, S.; Nagaraj, R. *J. Peptide Sci.* **2009**, *15*, 675–684.
- (72) Dwyer, D. S.; Bradley, R. J. *Cell. Mol. Life Sci.* **2000**, *57*, 265–275.
- (73) Dwyer, D. S. *Biopolymers* **1999**, *49*, 635–645.
- (74) Buck, M. Q. *Rev. Biophys.* **1998**, *31*, 297–355.
- (75) Munishkina, L. A.; Phelan, C.; Uversky, V. N.; Fink, A. L. *Biochemistry* **2003**, *42*, 2720–2730.
- (76) Perham, M.; Liao, J.; Wittung-Stafshede, P. *Biochemistry* **2006**, *45*, 7740–7749.
- (77) Yamaguchi, K.-i.; Naiki, H.; Goto, Y. *J. Mol. Biol.* **2006**, *363*, 279–288.
- (78) Dzwolak, W.; Grudzielanek, S.; Smirnovas, V.; Ravindra, R.; Nicolini, C.; Jansen, R.; Lokszejn, A.; Porowski, S.; Winter, R. *Biochemistry* **2005**, *44*, 8948–8958.
- (79) Stathopoulos, P. B. *Proc. Natl. Acad. Sci. U.S.A.* **2003**, *100*, 7021–7026.
- (80) Roy, S.; Katayama, D.; Dong, A.; Kerwin, B. A.; Randolph, T. W.; Carpenter, J. F. *Biochemistry* **2006**, *45*, 3898–3911.
- (81) Zhang, D.; Zhang, C.; Zhang, F.; Hu, J. *Microsc. Res. Techn.* **2011**, *74*, 481–483.
- (82) Hall, D. J.; Mash, C. J.; Pemberton, R. C. *NPL Rep. Chem.* **1979**, *95*, 36.